NASA/TM—2003-212300 ARL–TR–2954

Design and Fabrication of High-Temperature, Radial Magnetic Bearing for Turbomachinery

Gerald Montague
U.S. Army Research Laboratory, Glenn Research Center, Cleveland, Ohio

Mark Jansen, Ben Ebihara, and Ralph Jansen
University of Toledo, Toledo, Ohio

Alan Palazzolo, Randy Tucker, Jason Preuss, and Andrew Hunt
Texas A&M University, College Station, Texas

Jeff Trudell and Andrew Provenza
Glenn Research Center, Cleveland, Ohio

July 2003

The NASA STI Program Office . . . in Profile

Since its founding, NASA has been dedicated to the advancement of aeronautics and space science. The NASA Scientific and Technical Information (STI) Program Office plays a key part in helping NASA maintain this important role.

The NASA STI Program Office is operated by Langley Research Center, the Lead Center for NASA's scientific and technical information. The NASA STI Program Office provides access to the NASA STI Database, the largest collection of aeronautical and space science STI in the world. The Program Office is also NASA's institutional mechanism for disseminating the results of its research and development activities. These results are published by NASA in the NASA STI Report Series, which includes the following report types:

- TECHNICAL PUBLICATION. Reports of completed research or a major significant phase of research that present the results of NASA programs and include extensive data or theoretical analysis. Includes compilations of significant scientific and technical data and information deemed to be of continuing reference value. NASA's counterpart of peer-reviewed formal professional papers but has less stringent limitations on manuscript length and extent of graphic presentations.

- TECHNICAL MEMORANDUM. Scientific and technical findings that are preliminary or of specialized interest, e.g., quick release reports, working papers, and bibliographies that contain minimal annotation. Does not contain extensive analysis.

- CONTRACTOR REPORT. Scientific and technical findings by NASA-sponsored contractors and grantees.

- CONFERENCE PUBLICATION. Collected papers from scientific and technical conferences, symposia, seminars, or other meetings sponsored or cosponsored by NASA.

- SPECIAL PUBLICATION. Scientific, technical, or historical information from NASA programs, projects, and missions, often concerned with subjects having substantial public interest.

- TECHNICAL TRANSLATION. English-language translations of foreign scientific and technical material pertinent to NASA's mission.

Specialized services that complement the STI Program Office's diverse offerings include creating custom thesauri, building customized databases, organizing and publishing research results . . . even providing videos.

For more information about the NASA STI Program Office, see the following:

- Access the NASA STI Program Home Page at ***http://www.sti.nasa.gov***

- E-mail your question via the Internet to help@sti.nasa.gov

- Fax your question to the NASA Access Help Desk at 301–621–0134

- Telephone the NASA Access Help Desk at 301–621–0390

- Write to:
  NASA Access Help Desk
  NASA Center for AeroSpace Information
  7121 Standard Drive
  Hanover, MD 21076

NASA/TM—2003-212300 ARL–TR–2954

Design and Fabrication of High-Temperature, Radial Magnetic Bearing for Turbomachinery

Gerald Montague
U.S. Army Research Laboratory, Glenn Research Center, Cleveland, Ohio

Mark Jansen, Ben Ebihara, and Ralph Jansen
University of Toledo, Toledo, Ohio

Alan Palazzolo, Randy Tucker, Jason Preuss, and Andrew Hunt
Texas A&M University, College Station, Texas

Jeff Trudell and Andrew Provenza
Glenn Research Center, Cleveland, Ohio

National Aeronautics and
Space Administration

Glenn Research Center

July 2003

Acknowledgments

This research was funded by the NASA Glenn Smart Efficient Components (SEC) program, with Robert Corrigan the project manager, and a NASA Research Announcement with Texas A&M University. The authors wish to thank Paul Yedinak of Aircraft Finishing Systems for his wire insulation contribution and John Poles for his electrical support.

This report is a formal draft or working paper, intended to solicit comments and ideas from a technical peer group.

This report contains preliminary findings, subject to revision as analysis proceeds.

The Propulsion and Power Program at NASA Glenn Research Center sponsored this work.

Available from

NASA Center for Aerospace Information
7121 Standard Drive
Hanover, MD 21076

National Technical Information Service
5285 Port Royal Road
Springfield, VA 22100

Available electronically at http://gltrs.grc.nasa.gov

Design and Fabrication of High-Temperature, Radial Magnetic Bearing for Turbomachinery

Gerald Montague
U.S. Army Research Laboratory
National Aeronautics and Space Administration
Glenn Research Center
Cleveland, Ohio 44135

Mark Jansen, Ben Ebihara, Ralph Jansen
University of Toledo
Toledo, Ohio 43606

Alan Palazzolo, Randy Tucker, Jason Preuss, Andrew Hunt
Texas A&M University
College Station, Texas 77843

Jeff Trudell and Andrew Provenza
National Aeronautics and Space Administration
Glenn Research Center
Cleveland, Ohio 44135

Summary

Motors, magnetic bearings, and other electromagnetic actuators that can operate at 1000 °F (540 °C) hold great promise for providing increased efficiency in machinery for many applications ranging from pebble-bed nuclear reactors and chemical processing to aircraft and unmanned aerial combat vehicle (UCAV) propulsion systems. This report discusses in detail the design and fabrication of a high-temperature, heteropolar, radial magnetic bearing that was operated at 1000 °F (540 °C). The development of high-temperature wire and a coil fabrication process are two significant technical barriers overcome by the Army Research Laboratory (ARL), the NASA Glenn Research Center, and the Texas A&M University (TAMU) team. This is ARL/NASA/TAMU's third-generation high-temperature magnetic bearing. The motivation for this research came from the pursuit of a more electric gas turbine engine and a high-temperature, large-diameter, 4-million-DN (diam in millimeters times rotor speed in revolutions per minute) rotor support system.

Introduction

Currently, virtually all the engines that power aircraft use oil to lubricate the ball bearings. The maximum operating temperature of the rolling-element bearings is constrained because of lubricant temperature limits, typically less than 500 °F (270 °C). Therefore, a cooling system is used in many engines to keep the lubricant from degrading and detrimentally changing the antifriction properties. In addition to the bulky lubrication system, the cooling systems add additional weight and complexity to any propulsion system. The secondary air also robs the propulsion system of performance and complicates hardware. These are critical design considerations for programs such as the Joint Strike Fighter (JSF) and Long Range Bomber (LRB).

To reduce weight, part inventory, and maintenance time while at the same time increasing reliability, there has been an endeavor to replace hydraulic actuators with an electric equivalent. Almost all of today's modern aircraft already include electric actuators for several systems, and the push has

been for even more electric future aircraft. In 1998 an all-electric actuation system on an F–16 fighter underwent ground testing (ref. 1). This same motivation has been directed toward increasing reliability and decreasing weight in auxiliary power units (APU) and gas turbine engines.

Since these future aircraft will have much greater electrical requirements, larger APUs will be needed. These requirements may be met by operating larger systems at higher temperatures and speeds. Magnetic bearings provide an excellent alternative to conventional oil-lubricated ball bearings and allow the engine to use larger rotating components and to operate at much higher speeds and temperatures. All these factors will lead to a more efficient, higher power gas turbine engine.

An important consideration for a high-temperature magnetic bearing is the behavior of the soft magnetic material at elevated temperature. In 1967, Westinghouse Electric performed some of the first research on mechanical and magnetic properties of soft materials at extreme temperatures (ref. 2). Test data were evaluated for eight selected materials to be used in high-temperature electric devices. These data provided valuable information about heat-treatment effects and tradeoffs for mechanical versus magnetic performance.

More recently, Dr. Fingers from the U.S. Air Force Research Laboratory performed tests that supported the more electric aircraft effort (ref. 3). Until the documentation of Dr. Finger's tensile and creep test results, little data existed to describe the effect of thermal cycling or long periods of exposure at extreme temperatures on the mechanical properties of soft magnetic materials.

In 1997, Scholten (ref. 4) presented a practical control system design for a magnetically supported rotor that would operate at high speed (22 000 rpm) and high temperature (1000 °F or 540 °C). His work presented test data and simulations of adequate rotor stability under normal loads.

Mekhiche briefly described the design, fabrication, and testing of a high-temperature magnetic bearing operating at 50 000 rpm (ref. 5). However, this publication contains no coil technology information or test data at 1100 °F (593 °C).

Xu gave the results of a high-temperature magnetic bearing research program that included an investigation of materials and high-temperature displacement sensor development (ref. 6). In this investigation, 27-percent nickel-clad copper wire was used. However, he did not discuss the electrical resistance change at high temperature resulting from the nickel diffusion into the copper. Also, the coil packing factor and insulation process were not addressed. These parameters are discussed herein.

The objective of this report is to examine design and fabrication issues of a high-temperature magnetic bearing. A successful design and fabrication process are discussed. Load and power measurements for a complete range of speeds and temperatures for the magnetic bearing described herein can be found in references 7 and 8.

Modular C-Core Bearing Design

One major design criterion for this magnetic bearing was to maximize the force capacity, which was achieved by meeting two major design requirements: maximizing the pole coverage over the rotor laminations and maximizing the coil turns.

If the stator lamination back-iron leg were designed as one continuous ring, a common heteropolar design, the coils would have to be hand wound in place versus being wound on a bobbin, making the bearing construction extremely difficult. The advantage of the continuous back-iron is to give the bearing mutual inductance (flux path through failed coil poles), which enables fault tolerance if the coils are independently powered. However, if the bearing were designed with a continuous back-iron, it would eliminate any possibility of an easily automated coil winding process.

This limitation was overcome by choosing a modular design, which eliminates much of the handling strain during coil winding. In the modular design, each module contains two poles in "C" shape. The wire is wound on both poles continuously, eliminating many connections. The wire winding is described later in the section Coil Winding. The modular design reduces the winding labor and the possibility of nicking the insulation from excessive handling. The design also allows easy replacement of components. A disadvantage of this design is the elimination of the mutual inductance

seen with a continuous back-iron design. However, fault tolerance can still be achieved by the use of redundant axes.

The material used for the stator laminations is Hiperco 50,[1] an iron-cobalt-vanadium soft magnetic alloy that possesses high magnetic saturation and high maximum permeability. This alloy exhibits magnetic properties superior to those of other commercial iron-cobalt soft magnetic alloys (ref. 9).

Figure 1 shows the C-core Hiperco 50 lamination stack. The individual laminations are heat treated to maximize flux saturation and oxidation for electrical isolation. The 0.014-in.-(0.356-mm-) thick lamination reduces the eddy current losses generated in the stack. The unique features of this design are the small radii at the pole corners and the dovetail back-pole leg.

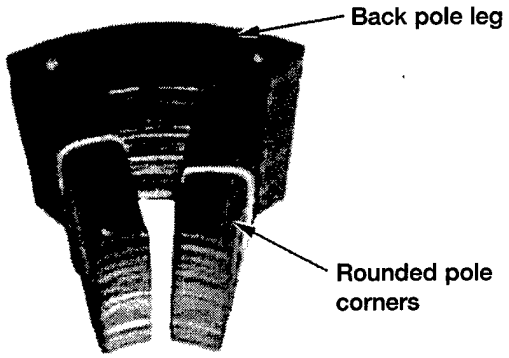

Figure 1.—Hiperco 50 laminated C-core stack.

Wire and Coil Construction

Wire Design Criteria

For a high-temperature bearing, special wire is required to meet conductor and insulation challenges. The wire conductor challenges include low resistance change as a function of temperature and resistance to oxidation. Bare copper wire was not used for this application because it oxidizes at high temperatures. Nickel-coated copper was not used because of the diffusion issue previously discussed. Commercially available, ceramic-coated wire was tested and was not used because of the thin, easily scratched coating. These scratches in the insulation would become numerous and result in coil turn-to-turn or coil conductor-to-lamination shorts. Instead, commercially available, 99.9-percent-pure, round, 18-gage, annealed silver wire was chosen. Silver is a good electrical conductor, does not oxidize easily, and is more pliable. Test results showed a lower resistance at extreme temperatures than copper, which reduced the i^2R losses (where i is current and R is electrical resistance).

The wire insulation must meet many different and stringent requirements. First, it must maintain its dielectric integrity during many thermal cycles and long exposure at high temperature. Second, the insulation must have good adhesion to the silver and not crack or flake off because of thermal expansion. Third, it must be pliable to allow for small radii turns during the coil winding process. Also, because the wire is in tension during the coil winding process, the insulation must have good tensile strength. Since the wire may come into contact with a number of rollers and bobbins during the coil winding where the insulation could easily be nicked, scratched, or worn away, the insulation must have good toughness and scratch resistance. Finally, microfretting between adjacent wires within the coil may occur during magnetic bearing operation, so insulation with good antifriction properties is desirable.

To achieve high current density within the coil, the volume of the wire conductor should be maximized within the coil volume. The packing factor is the ratio of the conductor cross-sectional area to the insulated wire area. The goal is to minimize the coil insulation and the voids between insulated wires created from the winding process. A packing factor close to the value of one is ideal but is physically impossible. Commercially available high-temperature wire is offered in a tubular

[1]Carpenter Technology Corporation is the registered owner of Hiperco 50.

sheath filled with an insulating medium. This is effective but not practical for electric coil applications requiring small volume (high packing factor). In pursuit of high-temperature wire, the authors used a commercially available, two-compound, clear ceramic coating.

Wire Insulation Process

To remove oxides and other contaminates from the surface of the silver wire, it is first cleaned using a light abrasive cleaning pad. To remove any oil and residual cleaning material, the wire is wiped with a clean cloth soaked in lacquer thinner. Next, the first ceramic coating is wiped onto the wire and it is then cured at 180 °F (82 °C) for 10 sec. The wire proceeds to the next station, where a second coating is applied and cured. The process is repeated a third time, leaving the wire triple coated. Subsequently, the wire continues through an air-cooling station, bringing it back to room temperature. Upon completion of the final coating process, the wire undergoes an electrical continuity test to check the integrity of the insulation coating. If any discrepancies are found, the wire is heated again and a fourth coat of insulation is applied. The final step entails having the wire triple S-glass wrapped by a commercial vendor.

The first coating is approximately 90 percent successful in insulating the wire. The second coat is applied to ensure complete coverage, and the third coating is an added factor of safety against failures. This process was also tested on square and ribbon-shaped conductors. However, the corners on the square wire did not coat satisfactorily and a nonuniform effect was observed on the ribbon material, leaving uncoated edges. The test schedule did not permit these coating issues to be pursued.

The outside diameter of the 18-gage silver wire was initially 0.040 in. (1.01 mm). After the triple ceramic coating, the outside diameter increased to 0.041 in. (1.04 mm). The final outside diameter of the triple-S-glass-wrap insulated wire was 0.060 in. (1.52 mm) and the resulting conductor-to-total-wire cross section was 0.67. A patent-pending, high-temperature wire insulating process was developed.

Coil Winding

The high pole-face coverage design did not allow the coils to be wound on a bobbin and then slipped onto the pole. The radii on the C-core lamination pole legs (fig. 2) prevent sharp knife edges from cutting into the wire insulation. The hand-winding fixture shown in figure 3 was developed to rotate a C-core lamination stack. Before winding, the poles are insulated using a high-temperature tape (fig. 4). The windings are stepped to form a taper from front to back to maximize the turns (fig. 5). The C-core has a north and south pole, with 52 coil turns per pole. One coil is wound completely; then, without cutting the wire, the winding direction is reversed and the second coil is wound.

Coil Potting Process

The coil windings are encapsulated and bonded with an alumina-based ceramic potting compound using an injection mold procedure. The maximum operating temperature of the compound is 3000 °F (1650 °C). Figure 6 shows the mold components used in the coil potting process. The potting compound injection molding device that was developed is shown in figure 7. Figure 8 is a photograph of a finished C-core.

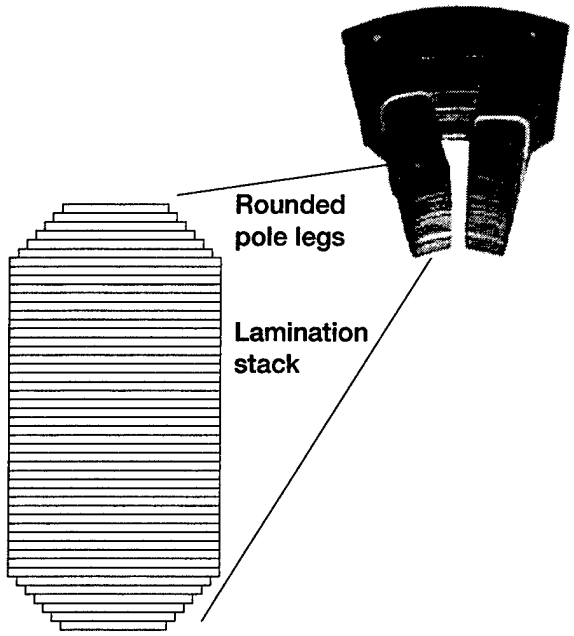

Figure 2.—End view of C-core pole showing tapering lamination stack for rounded poles.

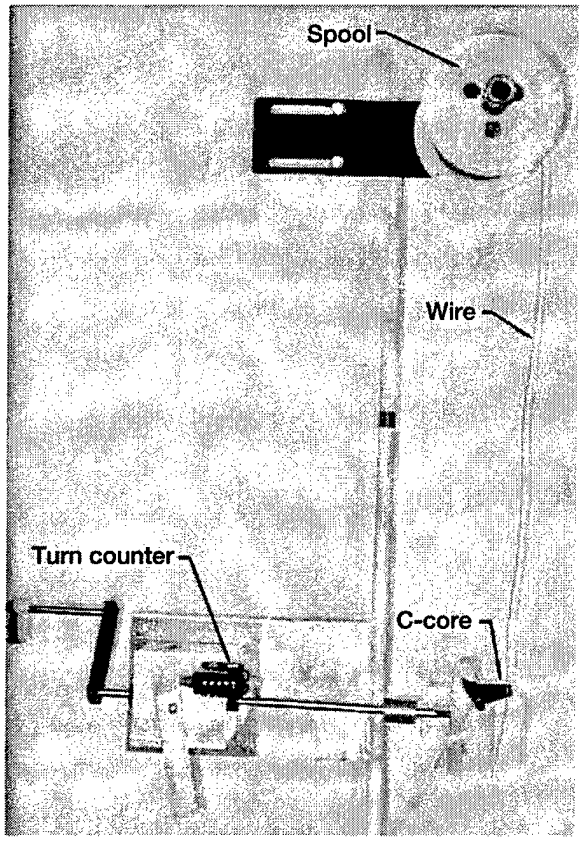

Figure 3.—Manual C-core coil winding mechanism.

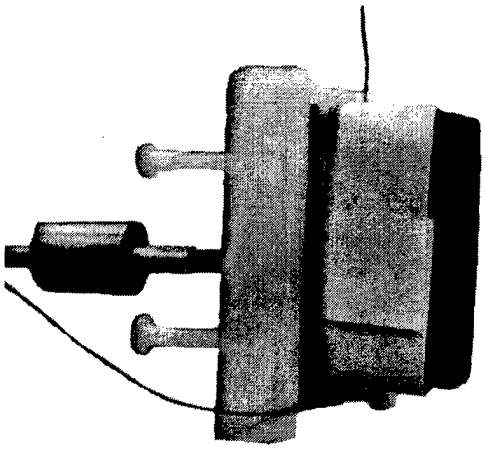

Figure 4.—High-temperature pole insulation.

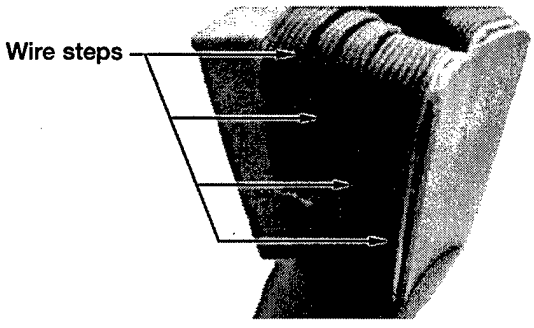

Figure 5.—Stepped-down tapered coil winding.

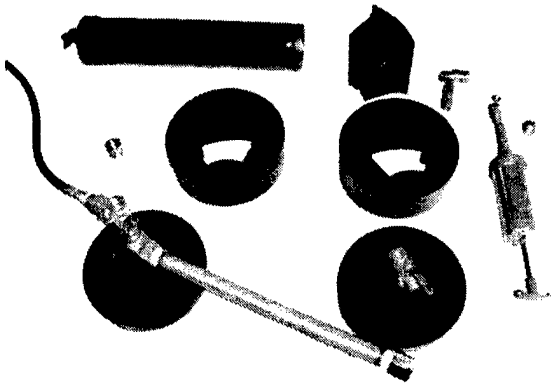

Figure 6.—Coil injection mold components.

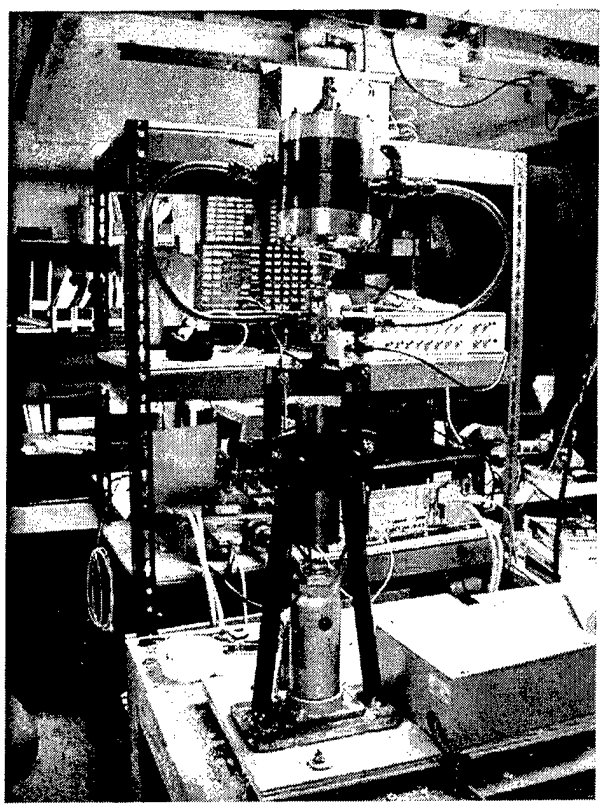

Figure 7.—Ceramic-compound coil injection mold machine.

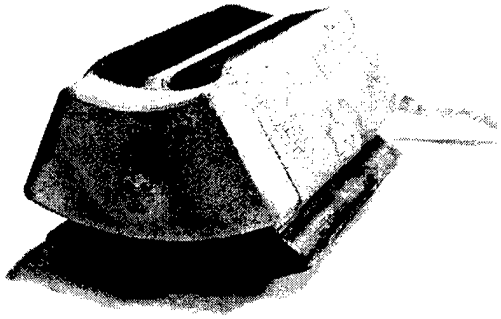

Figure 8.—Finished C-core.

Finished Coil Testing

Coil Resistance Versus Temperature Test

After the C-cores were completed, testing was done to ensure that no wires were damaged during assembly. The first test checked the resistance of each C-core up to 1000 °F (540 °C) by measuring the wire-to-wire dielectric integrity. A typical result is shown in figure 9. A failure in conductor insulation would result in a nonlinear (decrease in resistance) graph.

Coil Megger Test

The purpose of performing an insulation resistance test is to verify that the coil winding-to-lamination is not shorted. Insulation resistance readings are relative to environment and can differ from test to test on the same specimen, yet not indicate insulation breakdown. The important indicator is the trend in readings over a time period; a decreasing trend is a warning of insulation deterioration. Insulation resistance tests are performed using a Megger, which applies a known voltage and measures the resistance between what is connected between its terminals. For this test, one of the Megger leads is connected to one coil lead and the other to a conductive path on the lamination stack. This test checks for shorting between the coil wire and the lamination stack under a voltage load at test temperature (fig. 10).

Another method of testing, the time-resistance method, is fairly independent of temperature and can give conclusive information without records of previous tests. It is based on the absorption effect of good insulation compared with that of moist or contaminated insulation. Good insulation shows a continual increase in resistance over a period of time (5 to 10 min). The ratio of two time-resistance

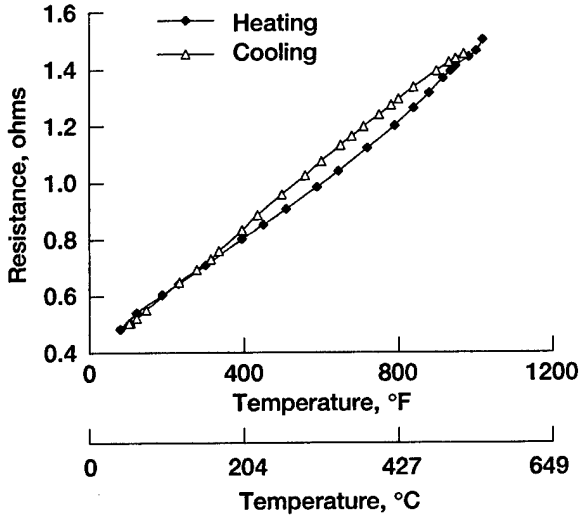

Figure 9.—Coil wire resistance versus temperature.

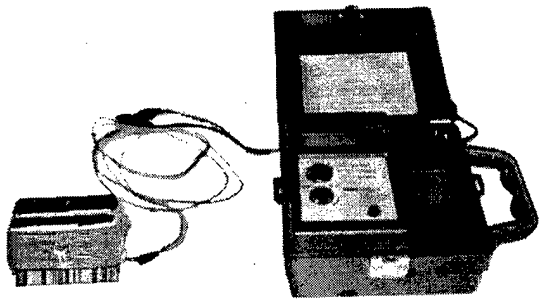

Figure 10.—Example of coil Megger test.

readings (a 10-min reading divided by a 1-min reading) is called the polarization index. Another typical insulation resistance test is the short-time (spot-reading) test, in which the Megger is operated for a short, specific time period (60 sec). The ratio of two time-resistance readings (60-sec reading divided by a 30-sec reading) is called the dielectric absorption ratio. Table I gives values of the ratios and corresponding relative conditions of the insulation.

Values approximately 20 percent higher than those shown in the table indicate a dry, brittle winding that will fail under shock conditions or during starts. The six C-cores tested fell into the good insulation range for both methods.

TABLE I.—INSULATION CONDITION[a]

Insulation condition	Polarization index	Dielectric absorption ratio
Poor	<1	<1
Questionable	1.0 to 2.0	1.0 to 1.4
Good	2.0 to 4.0	1.4 to 1.6
Excellent	>4.0	>1.6

[a]Standards are satisfactory for equipment with very low capacitance.

C-Core Support Ring and Rotor Lamination Design

C-Core Support Ring

To accommodate the modular C-core design, a C-core structural support ring had to be fabricated. The support ring provides the mounting structure for the C-core modules. To minimize flux leakage and match the thermal expansion coefficients of the C-core lamination material, Inconel 718 was used. The modular design allows for easy C-core replacement in the event of a coil failure. Each dovetail slot was individually machined to match the profile of a specific C-core. Although this design eliminates the flux paths to dead poles used in mutually inductive fault-tolerant control schemes, fault tolerance with this design has been demonstrated by utilizing a third control axis and a General Electric (GE) type control method. Figure 11 shows the completed support ring.

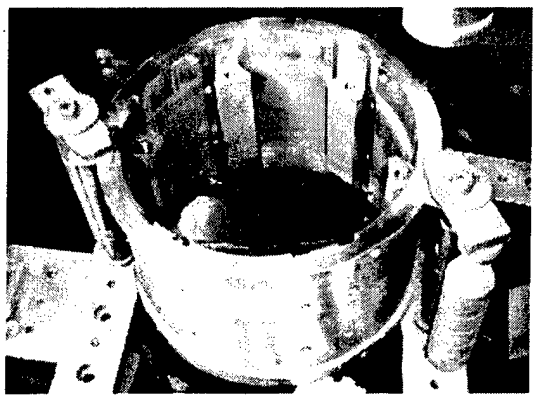

Figure 11.—Dovetailed Inconel 718 support ring.

Finite-Element Analysis

Because a magnetic axis is capable of producing over 1000 lb (4.45 kN) of force, several support ring design issues were addressed before manufacturing. One was the structural deflection of the ring and tabs under load at elevated temperatures. The reaction force of the C-core is applied across the tab surfaces between adjacent C-cores. A two-dimensional stress analysis was performed to predict ring deflection and stress under load and at temperatures up to 1000 °F (540 °C). If the ring were to morph out of round or if the C-core support tabs deflected, the air gap between the pole face and the rotor would be compromised, thus inducing uncertainties in the magnetic bearing force measurement. The force capacity of this bearing is inversely proportional to the square of the air gap, which is nominally 0.020 in. (0.5 mm) at 70 °F (21 °C).

The C-core support ring has an 8.0-in. (203-mm) outside diameter, a 7.2-in. (183-mm) inside diameter, and a 6.0-in. (152-mm) inner tab diameter. Each tab is spaced 60° apart. The slots next to the tab are used to place spacers to adjust C-core alignment. The slots have a 7.5-in. (190-mm) outside diameter with a 0.05-in. (1.3-mm) fillet radius and a 0.02-in. (0.5-mm) radius at the opposite side. The support ring model was simplified by neglecting the C-core to conservatively estimate displacements. Forces were applied directly to each of the nodes of the stator tab in contact with the C-core in the radial direction. The applied nodal force was calculated by dividing the total C-core force by 2, by the lamination stack length of 3.4 in. (86 mm), and by the number of nodes along the stack length. The physical and mechanical properties of the support ring material are given in table II.

The displacement of a tab with one 1000-lb (4.45-kN) actuator active at 1000 °F (540 °C) is shown in figure 12. The 1000-lb (4.45-kN) load causes tab rotation of approximately 0.001 in. (0.0254 mm), closer to the laminations at one end tab and farther at the other end. The structural ring displacements and stresses are summarized in table III for single- and dual-acting C-cores for 70 °F (21 °C) and 1000 °F (540 °C). Note that the displacement is dominated by the thermal expansion coefficient at 1000 °F (540 °C) and the stresses are significantly below yield strength. When stiffness effects of the C-core are included, the stress results indicate that a significant amount of structural ring weight reduction may be possible during redesign.

TABLE II.—PHYSICAL AND MECHANICAL PROPERTIES OF INCONEL 718

Density, lb/in.^{3} (g/cm^3)	0.296 (8.19)
Modulus of elasticity, psi (MPa) at	
70 °F (21 °C)	29.8×10^6 (20.5×10^4)
1000 °F (540 °C)	25.3×10^6 (17.4×10^4)
Poisson's ratio	0.28
Thermal expansion, in./(in./°F)$\times10^{-6}$ (cm/(cm/°C)) at	
70 °F (21 °C)	5.9 (1.76)
1000 °F (540 °C)	8.2 (2.46)
Yield strength (382 Brinnell hardness)	
below 1300 °F (704 °C), psi (MPa)	171×10^6 (11.8×10^5)

TABLE III.—STRUCTURAL RING DISPLACEMENT AND STRESS

C-core force, lbf (kN)		Temperature, °F (°C)	Displacement, in. (mm)		Von Mises stress, ksi (MPa)
Upper	Lower		Inside diameter	Outside diameter	
0 (0)	0 (0)	1000 (540)	0.0229 (0.582)	0.0305 (0.775)	—
1000 (4.45)	0 (0)	70 (21)	±.0009 (.0229)	.001 (.0254)	13 (89.6)
1000 (4.45)	0 (0)	1000 (540)	.0218 to .0236 (.553 to .599)	.0317 (.805)	13 (89.6)
1000 (4.45)	1000 (4.45)	1000 (540)	.0225 (.572)	.0306 (.777)	8 (55.16)
1000 (4.45)	1000 (4.45)	70 (21)	−.0003 (.0076)	.0001 (.0025)	8 (55.16)

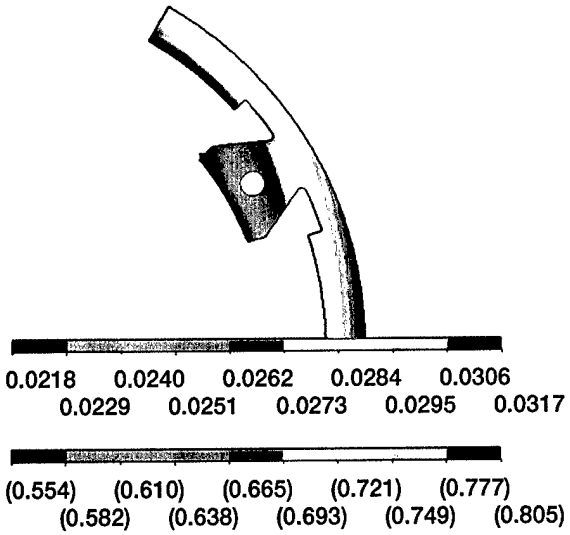

Figure 12.—ANSYS C-core support ring displacement, in. (mm).

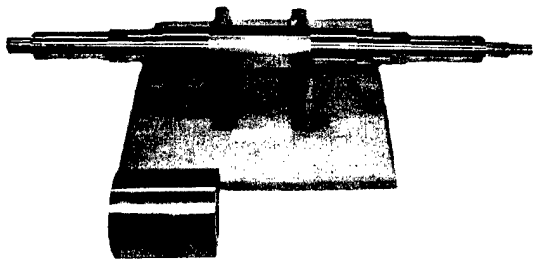

Figure 13.—Inconel 718 rotor with splined Hiperco 50 HS lamination stack.

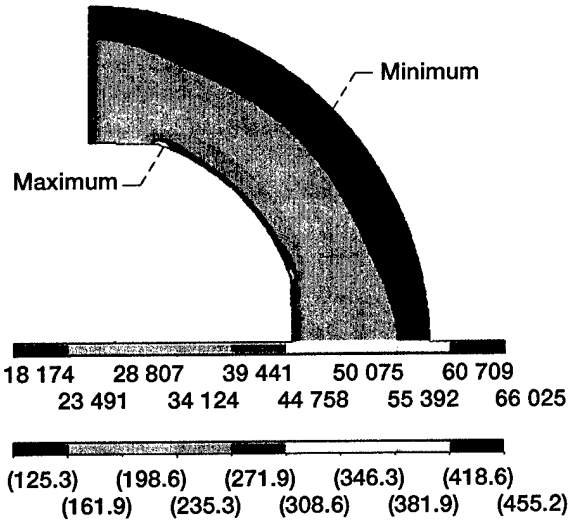

Figure 14.—Rotor lamination stress, psi (MPa).

Rotor Laminations

Hiperco 50 HS,[2] used for the rotor lamination material, is a variation of Hiperco 50 A,[3] which contains small additions of niobium and carbon for increased mechanical strength. These additions cause only a small reduction in the magnetic properties of the material (ref. 9). Figure 13 shows the finished rotor and lamination stack. The keyed rotor lamination stack has a nominal 2.96-in. (75-mm) outside diameter, a 1.80-in. (45.6-mm) inside diameter, and a 1.70-in. (43-mm) flat distance as shown in figure 14. There was no fillet radius between the flat and inside diameter. The Hiperco 50 HS

[2]Carpenter Technology Corporation is the registered owner of Hiperco 50 HS.
[3]Carpenter Technology Corporation is the registered owner of Hiperco 50 A.

physical and mechanical properties are given in table IV. The laminations were heat treated to a 99-ksi (682-MPa) yield strength. The Von Mises stress at 48 000 rpm and 70 °F (21 °C) is 66 ksi (455.1 MPa) as shown in figure 14. From figure 4.8 of reference 5, the average lower yield strength of Hiperco 50 HS at 1000 °F (540 °C) is approximately 80 ksi (551 MPa).

If a safety factor of 1.2 is applied, the laminations have a positive margin at 48 000 rpm, significantly above the 30 000-rpm test speed. The rotor lamination displacement and stresses are summarized in table V. A comparison of tables IV and V shows that the mismatch between the support ring and rotor lamination thermal expansion coefficients has increased the nominal gap by approximately 0.014 in. (0.356 mm) at 1000 °F (540 °C). If a fillet were added between the lamination flat and inside diameter, the stress concentration could be reduced by 30 percent.

TABLE IV.—PHYSICAL AND MECHANICAL PROPERTIES OF HIPERCO 50 HS

Density, lb/in.^{3} (g/cm^3)	0.293 (8.11)
Modulus of elasticity, psi (MPa)	30×10^6 (20.7×10^4)
Poisson's ratio	0.33
Thermal expansion, in./(in./°F)$\times10^{-6}$ (cm/(cm/°C)) at	
70 °F (21 °C)	5.3 (1.59)
1000 °F (540 °C)	5.9 (1.76)

TABLE V.—ROTOR LAMINATION DISPLACEMENT AND STRESS

Speed, krpm	Temperature, °F (°C)	Displacement, in. (mm)		Von Mises stress, ksi (MPa)
		Inside diameter	Outside diameter	
0	1000 (540)	0.0047 (0.119)	0.0081 (0.206)	—
48	1000 (540)	.0059 (.150)	.0091 (.231)	66 (455.1)

Stator Mounting in Test Facility

The mounting of the stator in the test facility is not trivial. The need to accommodate radial and axial thermal expansion of the stator while maintaining concentricity with the rotor is required. The structural integrity of the ring support mechanism had to maintain its position at 1000 °F (540 °C) with 1000-lb (4.45-k N) loads applied.

The final solution was to support the stator at eight locations with off-center rollers. Four rollers are mounted on each side of the stator, each roller mounted 90° apart from the other and 45° off the true vertical and horizontal axis. This configuration is shown in figure 15.

The test facility support frame is made from 1.0-in.- (25-mm-) thick steel welded plates, which prevent thermal and structural deflection under load. Two 0.5-in. (13-mm) face plates are mechanically fastened to the support frame. The plates have four slots machined to house the off-center rollers. The support plate and rollers are fabricated from the same material to match thermal expansion rates.

The rollers are 0.5-in.- (13-mm-) long cylinders with an off-center hole through them. A bolt is put through the roller and threaded into the C-core support ring. The stator is axially and radially aligned. The rollers are then tightened down to the support ring. Each roller provides two friction line contacts that enable alignment, prevent position change under load, and allow radial and axial thermal expansion of the ring.

At the date of this publication (5/22/2003), this radial magnetic bearing had been operated over 29 hr at 1000 °F (540 °C) during 18 thermal cycles (fig. 16).

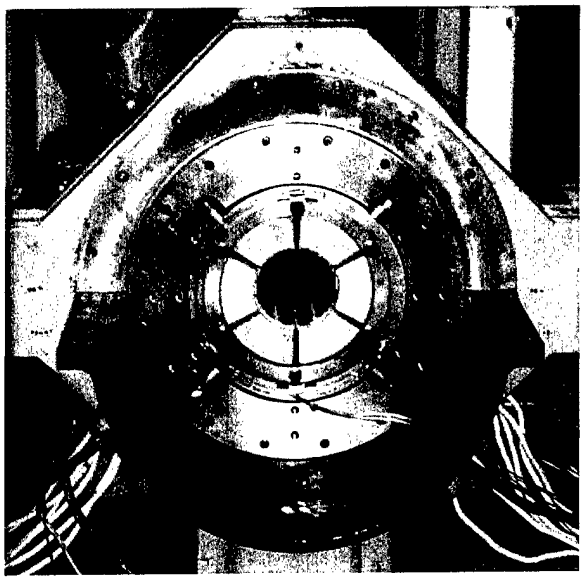

Figure 15.—Stator installed in NASA Glenn test facility.

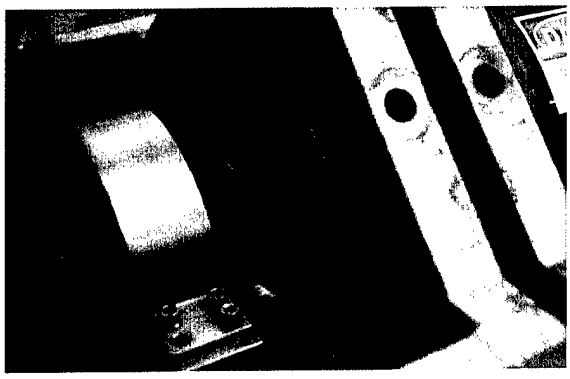

Figure 16.—Magnetic bearing operating at 1000 °F (540 °C).

Conclusion

This report addresses magnetic bearing design issues for a high-temperature application. The issues include stator deflections and stresses, stator mounting, rotor lamination stresses, and modular construction to maximize force. The modular design enables easy replacement of magnet cores. Due to the width limitations of the lamination material available from venders, this stator design enables the fabrication of much larger diameter magnetic bearings.

Detailed information was given on the development of a high-temperature wire insulation process and coil construction with a higher packing factor and scratch resistance than what was available commercially. A process to fabricate and test an electromagnetic bearing at 1000 °F (540 °C) was also described. In addition, the magnetic bearing had successfully been operated for hundreds of hours at temperatures ranging from room to 1000 °F (540 °F).

Future work includes using this high-temperature magnetic bearing as a static and dynamic load applicator to evaluate a high-temperature hydrostatic bearing rotor support system at elevated temperatures and high speed. Force and power measurements versus temperature and rotational speed for a high-temperature magnetic thrust bearing will also be completed.

References

1. All-Electric F–16 Ground Testing Goes Ahead, Flight International 4–10, p. 17, Nov. 1998.
2. Kueser, P., et al.: Properties of Magnetic Materials for Use in High Temperature Space Power Systems, NASA SP–3043, 1967.
3. Fingers, R.: Creep Behavior of Thin Laminations of Iron-Cobalt Alloys for Use in Switched Reluctance Motors and Generators, AFRL–PR–WP–TR–1999–2053, June 1999.
4. Scholten, J.R.: A Magnetic Bearing Suspension System for High Temperature Gas Turbine Applications: Control System Design, International Gas Turbine and Aeroengine Congress and Exhibition, Orlando, Florida, June 1997.
5. Mekhiche, M., et al.: 50,000 RPM, 1100 °F Magnetic Bearings for Jet Turbine Engines, Seventh Inter. Symp. On Mag. Brgs, ETH Zurich, August 2000.
6. Xu, L.; Wang, L.; and Schweitzer, G.: Development of Magnetic Bearings for High Temperature Suspension, Seventh Inter. Symp. On Mag. Brgs, ETH Zurich, August 2000.
7. Montague, G., et al.: Room Temperature Characterization of a Magnetic Bearing for Turbomachinery, NASA\TM—2002-211904 and ARL–TR–2858, 2002.
8. Montague, G., et al.: High Temperature Characterization of a Magnetic Bearing for Turbomachinery, NASA\TM—2003-212183 and ARL–TR–2929.
9. High Temp Metals, Inc., Hiperco Alloy Materials Property Sheet, Retrieved December 10, 2002, http://www.hightempmetals.com/hitempPermendurdata.html

REPORT DOCUMENTATION PAGE

Form Approved
OMB No. 0704-0188

1. AGENCY USE ONLY (*Leave blank*)	2. REPORT DATE	3. REPORT TYPE AND DATES COVERED
	July 2003	Technical Memorandum

4. TITLE AND SUBTITLE

Design and Fabrication of High-Temperature, Radial Magnetic Bearing for Turbomachinery

5. FUNDING NUMBERS

WBS–22–708–28–12
1L161102AF20

6. AUTHOR(S)

Gerald Montague, Mark Jansen, Ben Ebihara, Ralph Jansen, Alan Palazzolo, Randy Tucker, Jason Preuss, Andrew Hunt, Jeff Trudell, and Andrew Provenza

7. PERFORMING ORGANIZATION NAME(S) AND ADDRESS(ES)

National Aeronautics and Space Administration
John H. Glenn Research Center at Lewis Field
Cleveland, Ohio 44135–3191

8. PERFORMING ORGANIZATION REPORT NUMBER

E–13861

9. SPONSORING/MONITORING AGENCY NAME(S) AND ADDRESS(ES)

National Aeronautics and Space Administration
Washington, DC 20546–0001
and
U.S. Army Research Laboratory
Adelphi, Maryland 20783–1145

10. SPONSORING/MONITORING AGENCY REPORT NUMBER

NASA TM—2003-212300
ARL–TR–2954

11. SUPPLEMENTARY NOTES

Gerald Montague, U.S. Army Research Laboratory, NASA Glenn Research Center; Mark Jansen, Ben Ebihara, and Ralph Jansen, University of Toledo, Toledo, Ohio 43606; Alan Palazzolo, Randy Tucker, Jason Preuss, and Andrew Hunt, Texas A&M University, College Station, Texas 77843; Jeff Trudell and Andrew Provenza, NASA Glenn Research Center. Responsible person, Gerald Montague, organization code 0300, 216–433–6252.

12a. DISTRIBUTION/AVAILABILITY STATEMENT

Unclassified - Unlimited
Subject Categories: 07 and 37 Distribution: Nonstandard

Available electronically at http://gltrs.grc.nasa.gov

This publication is available from the NASA Center for AeroSpace Information, 301–621–0390.

12b. DISTRIBUTION CODE

13. ABSTRACT (*Maximum 200 words*)

Motors, magnetic bearings, and other electromagnetic actuators that can operate at 1000 °F (540 °C) hold great promise for providing increased efficiency in machinery for many applications ranging from pebble-bed nuclear reactors and chemical processing to aircraft and unmanned aerial combat vehicle (UCAV) propulsion systems. This report discusses in detail the design and fabrication of a high-temperature, heteropolar, radial magnetic bearing that was operated at 1000 °F (540 °C). The development of high-temperature wire and a coil fabrication process are two significant technical barriers overcome by the Army Research Laboratory (ARL), the NASA Glenn Research Center, and the Texas A&M University (TAMU) team. This is ARL/NASA/TAMU's third-generation high-temperature magnetic bearing. The motivation for this research came from the pursuit of a more electric gas turbine engine and a high-temperature, large-diameter, 4-million-DN (diam in millimeters times rotor speed in revolutions per minute) rotor support system.

14. SUBJECT TERMS

Turbomachinery; Dielectric insulation; Ceramic potting compound; Magnetic bearing; C-core

15. NUMBER OF PAGES

19

16. PRICE CODE

17. SECURITY CLASSIFICATION OF REPORT	18. SECURITY CLASSIFICATION OF THIS PAGE	19. SECURITY CLASSIFICATION OF ABSTRACT	20. LIMITATION OF ABSTRACT
Unclassified	Unclassified	Unclassified	